Available online at www.sciencedirect.com
ScienceDirect
Scripta Materialia 57 (2007) 125–128
Scripta MATERIALIA
www.elsevier.com/locate/scriptamat

Orientation relationship between C14 precipitate and (A2 + $D0_3$) matrix in an Fe–20at.%Al–8at.%Ti alloy

Chun-Wei Su,[a] Shiang-Cheng Jeng,[b] Chuen-Guang Chao[a] and Tzeng-Feng Liu[a,*]

[a] *National Chiao Tung University, 1001 Ta Hsueh Road, Hsinchu 30049, Taiwan*
[b] *Technology and Science Institute of Northern Taiwan, Taiwan*

Received 10 February 2007; revised 15 March 2007; accepted 16 March 2007
Available online 30 April 2007

When the Fe–20at.%Al–8at.%Ti alloy was aged at 1000 °C for 1 h and then quenched, the microstructure of the alloy was a mixture of (A2 + $D0_3$ + C14) phases. By means of transmission electron microscopy and diffraction techniques, the orientation relationship between the C14 precipitate and (A2 + $D0_3$) matrix was determined to be: $(0001)_{C14}\|(\bar{1}\bar{1}2)_m$, $(\bar{1}100)_{C14}\|(\bar{1}10)_m$, $(11\bar{2}0)_{C14}\|(111)_m$. This orientation relationship has not been reported in Fe–Al–Ti alloy systems before.

Keywords: Iron alloys; Electron diffraction; Transmission electron microscopy (TEM); C14 precipitate

The microstructures of the Fe–Al–Ti alloys have been studied by other workers [1–7]. In their studies, it is seen that only four phase fields, namely A2 (disordered body-centered cubic), A2 + $D0_3$, $D0_3$ and B2, could be found in the Fe–(18–25)at.%Al–Ti alloys with Ti $\leqq$ 5 at.% [1,2]. However, when the Ti content was increased to $\geqslant$7 at.%, C14 precipitates could be seen to form within the A2, A2 + $D0_3$, $D0_3$ or B2 matrix in the aged Fe–Al–Ti alloys [2–7]. The C14 precipitate has a hexagonal structure, with lattice parameters $a = 0.5038$ nm and $c = 0.8193$ nm [7]. Although the C14 precipitate was extensively reported to be detected in the aged Fe–Al–Ti alloys, little information concerning the orientation relationship between the C14 precipitate and matrix has been provided. Therefore, the purpose of the present study is to attempt to determine the orientation relationship between the C14 precipitate and (A2 + $D0_3$) matrix in the Fe–20at.%Al–8at.%Ti alloy.

The Fe–20at.%Al–8at.%Ti alloy was prepared in a vacuum induction furnace using 99.5% Fe, 99.9% Al and 99.7% Ti. The melt was chill cast into a $30 \times 50 \times 200$ mm^3 copper mold. After being homogenized at 1250 °C for 48 h, the ingot was sectioned into 2-mm-thick slices. These slices were subsequently solution heat-treated at 1250 °C for 2 h and then quenched rapidly in room-temperature water. The aging process was performed at 1000 °C for 1 h in a vacuum heat-treated furnace followed by further rapid quenched. Transmission electron microscopy specimens were prepared by means of a double-jet electropolisher with an electrolyte comprising 67% methanol and 33% nitric acid. The polishing temperature was kept in the range −30 to −20 °C, and the current density was kept in the range 4.0×10^4–6.0×10^4 A m^{-2}. Electron microscopy was performed on a JEOL JEM-2000FX scanning transmission electron microscope operating at 200 kV.

When the as-quenched alloy was aged at 1000 °C for 1 h and then quenched, rod-like precipitates were found to appear within the matrix. A typical example is shown in Figure 1a. Figure 1b is a selected-area diffraction pattern (SADP) taken from the matrix, exhibiting the superlattice reflection spots of the ordered $D0_3$ phase [8]. Figure 1c is a $(1\bar{1}1)$ $D0_3$ dark-field (DF) electron micrograph of the same area as Figure 1a, revealing the presence of extremely fine $D0_3$ domains. Figure 1d, a (002) DF electron micrograph, shows the presence of small B2 domains and a high density of disordered A2 phase (dark contrast) within the B2 domains. Since the sizes of both $D0_3$ and B2 domains are very small, it is deduced that the (A2 + $D0_3$) phases were formed by an A2 → B2 → (A2 + $D0_3$) ordering transition during quenching [9–12]. This result is similar to that observed by Mediratta et al. in the Fe–20at.%Al–5at.%Ti alloy

* Corresponding author. E-mail addresses: tfliu@cc.nctu.edu.tw; ian.mse86@nctu.edu.tw

1359-6462/$ - see front matter © 2007 Published by Elsevier Ltd. on behalf of Acta Materialia Inc.
doi:10.1016/j.scriptamat.2007.03.038

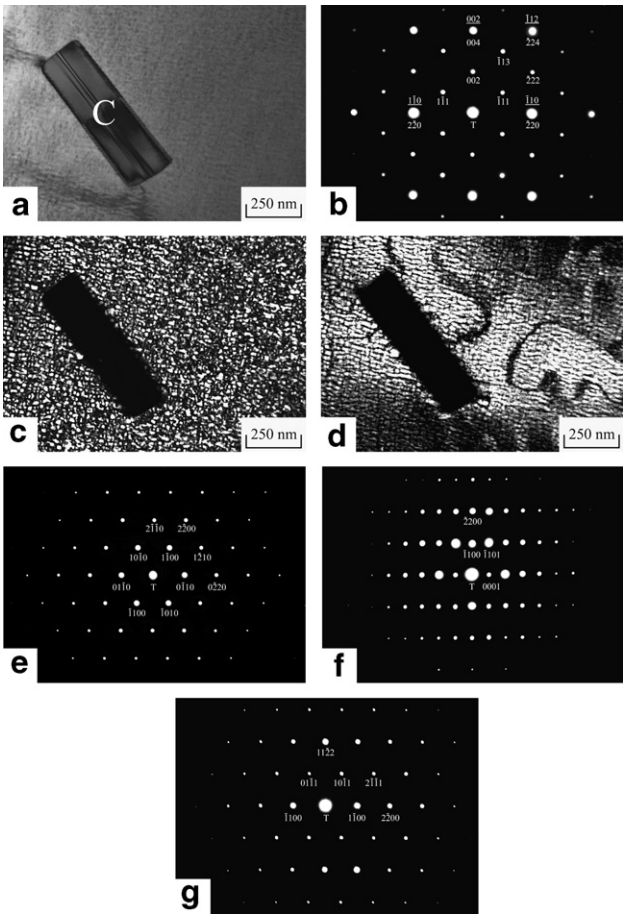

Figure 1. Electron micrographs of the alloy aged at 1000 °C for 1 h: (a) BF, (b) an SADP. The foil normal is [110]. $\underline{hkl}$ = A2 phase; hkl = $D0_3$ phase. (c) and (d) $(1\bar{1}1)$ and (002) $D0_3$ DF, respectively. (e–g) Three SADPs taken from the precipitate marked as "C" in (a). The zone axes of the C14 precipitate are (e) [0001], (f) $[11\bar{2}0]$ and (g) $[11\bar{2}\bar{3}]$, respectively.

quenched from 1100 °C [1]. In Figure 1b, it is seen that the orientation relationship between the A2 phase and the ordered $D0_3$ phase was $(002)_{A2}\|(002)_{D0_3}$ and $[110]_{A2}\|[110]_{D0_3}$. Figures 1e–g show three different SADPs taken from the rod-like precipitate marked as "C" in Figure 1a. According to the camera length and the measurement of the *d*-spacings as well as angles among the reciprocal lattice vectors of the diffraction spots, the crystal structure of the precipitate was determined to be hexagonal with lattice parameters $a = 0.505$ nm and $c = 0.801$ nm, which corresponds to that of the C14 phase [7]. The zone axes of the precipitate in Figure 1e–g are [0001], $[11\bar{2}0]$ and $[11\bar{2}\bar{3}]$, respectively. Based on the above examinations, it is concluded that the microstructure of the alloy aged at 1000 °C for 1 h and then quenched was a mixture of (A2 + $D0_3$ + C14) phases.

In order to determine the orientation relationship between the C14 precipitate and the (A2 + $D0_3$) matrix, six different SADPs were taken from an area including the precipitate marked as "C" in Figure 1a and its surrounding (A2 + $D0_3$) matrix. The results are shown in Figures 2a–f. The zone axes of the C14 precipitate and (A2+$D0_3$) matrix in Figures 2a–f are $[11\bar{2}0]_{C14}$, $[111]_m$; $[22\bar{4}\bar{3}]_{C14}$, $[110]_m$; $[11\bar{2}\bar{3}]_{C14}$, $[\bar{2}\bar{2}1]_m$; $[11\bar{2}\bar{6}]_{C14}$, $[\bar{1}\bar{1}1]_m$; $[0001]_{C14}$, $[\bar{1}\bar{1}2]_m$; and $[13\bar{5}\bar{8}\bar{6}]_{C14}$, $[100]_m$, respectively. It is obvious in Figures 2a and e that the (0001) and $(11\bar{2}0)$ reflection spots of the C14 precipitate are parallel to the $(\bar{1}\bar{1}2)$ and (111) reflection spots of the matrix, respectively. By means of this information, a stereographic plot of poles (superimposing the (0001) projection of the C14 precipitate and the $(\bar{1}\bar{1}2)$ projection of the matrix) was constructed, as shown in Figure 3, where the $(11\bar{2}0)$ pole of the C14 precipitate was made to match with the (111) pole of the matrix. In this stereographic plot, the interplanar angles between the chosen reciprocal reflections of the C14 precipitate were obtained by calculation using the following equation [13]:

$$\cos\phi = \frac{h_1h_2 + k_1k_2 + \frac{1}{2}(h_1k_2 + k_1h_2) + \frac{3a^2}{4c^2}l_1l_2}{\left\{\left(h_1^2 + k_1^2 + h_1k_1 + \frac{3a^2}{4c^2}l_1^2\right)\left(h_2^2 + k_2^2 + h_2k_2 + \frac{3a^2}{4c^2}l_2^2\right)\right\}^{\frac{1}{2}}}$$

It is clear in Figure 3 that the $(\bar{1}100)$, $(11\bar{2}4)$, $(11\bar{2}1)$ poles of the C14 precipitate would coincide with the $(\bar{1}10)$, (001), (112) poles of the matrix. These results are quite consistent with the observations of SADPs in Figure 2. On the basis of the preceding analyses, the orientation relationship between the C14 precipitate and (A2 + $D0_3$) matrix can be best stated as follows:

$$(0001)_{C14}\|(\bar{1}\bar{1}2)_m,\ (\bar{1}100)_{C14}\|(\bar{1}10)_m,\ (11\bar{2}0)_{C14}\|(111)_m$$

Finally, it is worthwhile mentioning that the C14 precipitate was also observed by many workers in Fe–Al–Nb, Fe–Al–Zr and Fe–Al–Ta alloys [5,14–16]. However, we are aware of only one article in which the orientation relationship between the C14 precipitate and the matrix was predicted. In 2005, Morris et al. reported that when the Fe–25Al–2Nb alloy was aged at 800 or 900 °C, C14 precipitates were formed within the $D0_3$ matrix; the orientation relationship between the C14 precipitate and $D0_3$ matrix was $\{\bar{1}010\}_{C14}\|\{\bar{1}01\}_m$, $\langle 1\bar{2}10\rangle_{C14} \approx \langle 010\rangle_m$ and $\langle 0001\rangle_{C14} \approx \langle 101\rangle_m$ [14]. Interestingly, it is noted here that the previous result of $\{\bar{1}010\}_{C14}\|\ \{\bar{1}01\}_m$ is indeed in agreement with that observed in Figure 2a of the present work. However, in the previous study [14], it was reported that the only exact relationship was $[\bar{1}010]_{C14}\|[\bar{1}01]_m$, all other relationships being approximate, with a difference of a few degrees (3–5°). Therefore, it is not clear whether the present orientation relationship is the same as that reported by Morris et al. for the Fe–25Al–2Nb alloy.

In summary, when the alloy was aged at 1000 °C for 1 h and then quenched, the microstructure of the alloy was a mixture of (A2 + $D0_3$ + C14) phases. The orientation relationship between the C14 precipitate and (A2 + $D0_3$) matrix can be best stated as follows:

$$(0001)_{C14}\|(\bar{1}\bar{1}2)_m,\ (\bar{1}100)_{C14}\|(\bar{1}10)_m,\ (11\bar{2}0)_{C14}\|(111)_m$$

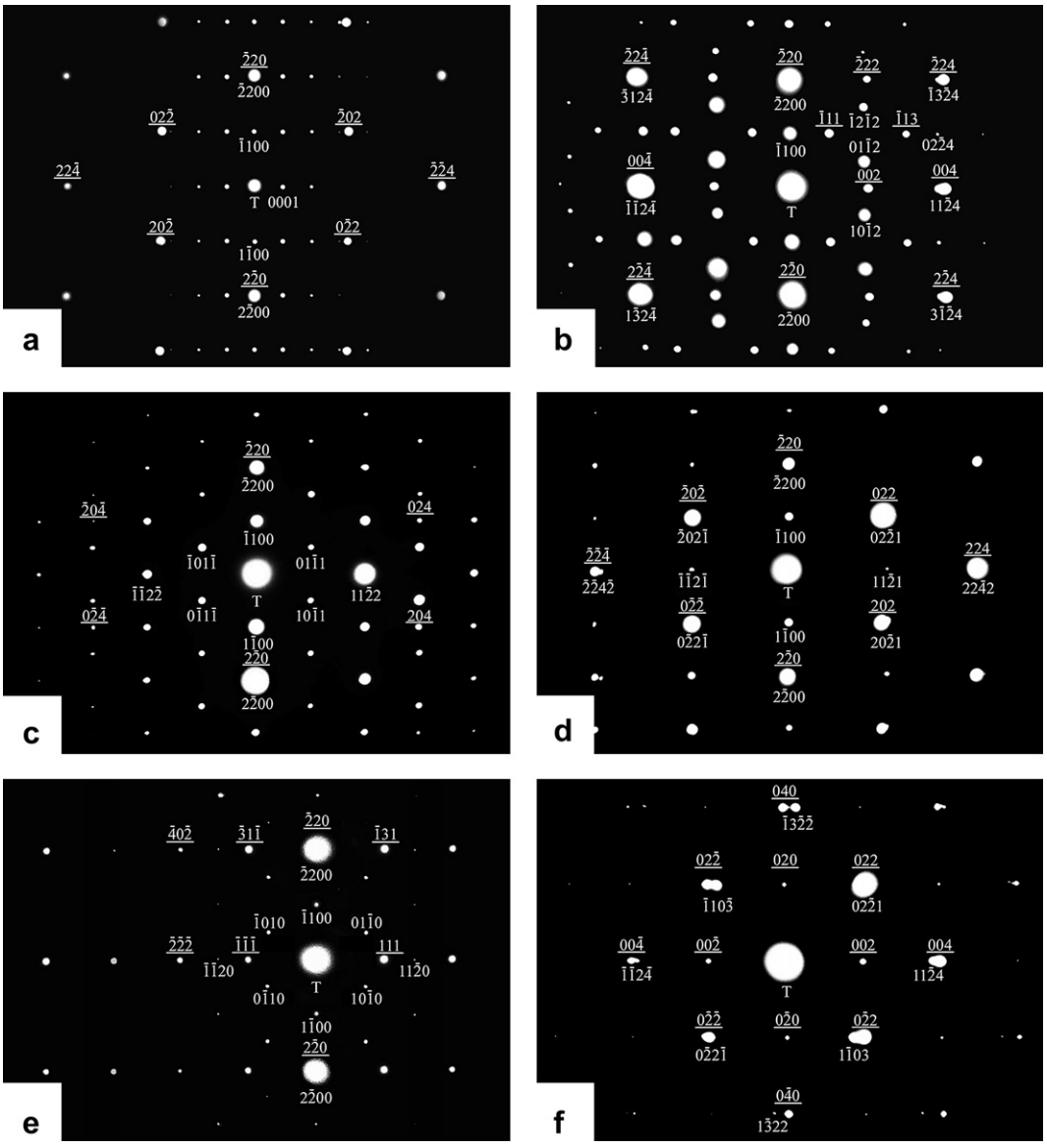

Figure 2. Six SADPs taken from an area including the precipitate marked as "C" in Figure 1a and its surrounding matrix. The zone axes of the (A2 + $D0_3$) matrix are (a) [1 1 1], (b) [1 1 0], (c) [$\bar{2}\,\bar{2}$ 1], (d) [$\bar{1}\,\bar{1}$ 1], (e) [$\bar{1}\,\bar{1}$ 2] and (f) [1 0 0], respectively. *hkil* = C14 precipitate; $\underline{hkl}$ = $D0_3$ phase.

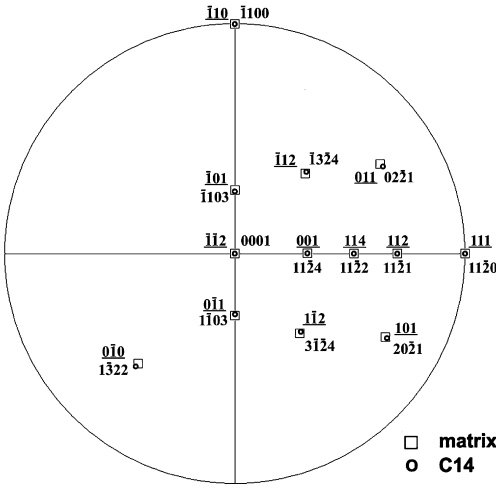

Figure 3. The superimposed C14/$D0_3$ stereogram describing the orientation relationship between the C14 precipitate and (A2 + $D0_3$) matrix.

We are pleased to acknowledge the financial support of this research by the National Science Council, Republic of China under Grant NSC95-2221-E-009-086-MY3. We are also grateful to M.H. Lin for typing the manuscript.

[1] M.G. Mediratta, S.K. Ehlers, H.A. Lipsitt, Metall. Trans. A 18 (1987) 509.
[2] C.H. Sellers, T.A. Hyde, T.K. O'Brien, R.N. Wright, J. Phys. Chem. Solids 55 (1994) 505.
[3] M. Palm, J. Lacaze, Intermetallics 14 (2006) 1291.
[4] U. Prakash, G. Sauthoff, Intermetallics 9 (2001) 107.
[5] M. Palm, Intermetallics 13 (2005) 1286.
[6] M. Palm, G. Sauthoff, Intermetallics 12 (2004) 1345.
[7] M. Palm, G. Inden, N. Thomas, J. Phase Equilib. 16 (1995) 209.
[8] C.H. Chen, T.F. Liu, Metall. Trans. A 34 (2003) 503.
[9] S.M. Allen, J.W. Cahn, Acta Metall. 24 (1976) 425.

[10] M.J. Marcinkowski, N. Brown, J. Appl. Phys. 33 (1962) 537.
[11] C.C. Wu, T.F. Liu, Metall. Trans. A 22 (1991) 1417.
[12] T.F. Liu, J.S. Chou, C.C. Wu, Metall. Trans. A 21 (1990) 1891.
[13] J.W. Edington, The Operation and Calibration of the Electron Microscope, vols. 1–5, MacMillan Press, London, 1985.
[14] D.G. Morris, L.M. Requejo, M.A. Muñoz-Morris, Intermetallics 13 (2005) 862.
[15] F. Stein, M. Palm, G. Sauthoff, Intermetallics 13 (2005) 1056.
[16] F. Stein, M. Palm, G. Sauthoff, Intermetallics 13 (2005) 1275.